

Technology development in support of hyperspectral infrared atmospheric sounding in a CubeSat

Thomas S. Pagano, Carlo Abesamis, Andres Andrade, Hartmut Aumann, Sarath Gunapala, Cate Heneghan, Robert Jarnot, Dean Johnson, Andy Lamborn, Yuki Maruyama, Sir Rafol, Nasrat Raouf, David Rider, Dave Ting, Dan Wilson, Karl Yee
Jet Propulsion Laboratory, California Institute of Technology
4800 Oak Grove Dr., Pasadena, CA 91109

Jerold Cole, Bill Good, Tom Kampe, Juancarlos Soto
Ball Aerospace and Technologies Corporation
Boulder CO, 80301

Arn Adams, Matt Buckley, Richard Graham, Fred Nicol, Tony Vengel,
John Moore, Thomas Coleman
IRCameras
Santa Barbara, CA 93103

Steve Schneider, Chris Esser, Scott Inlow, Devon Sanders, Karl Hansen,
Matt Zeigler, Charles Dumont, Rebecca Walter, Joe Piacentine
Blue Canyon Technologies
Boulder CO, 80301

ABSTRACT

Hyperspectral infrared sounding in a CubeSat will provide a new dimension to the current suite of IR sounders by allowing measurements at multiple times of day and enabling formation flying of IR sounders for new data products such as Atmospheric Motion Vector (AMV) winds. This paper focuses on technology development during the CubeSat Infrared Atmospheric Sounder (CIRAS) project sponsored by the NASA Earth Science Technology Office (ESTO), and coincident studies by the NOAA Office of Projects, Planning, and Analysis (OPPA). The CIRAS approach incorporates key new instrument technologies developed at JPL's Microdevices Lab (MDL) including a 2D array of High Operating Temperature Barrier Infrared Detector (HOT-BIRD) material, selected for its high uniformity, low cost, low noise and higher operating temperatures than traditional materials. The second key technology is an MWIR Grating Spectrometer (MGS) designed by Ball Aerospace with a JPL MDL slit and immersion grating to provide hyperspectral infrared imaging in a CubeSat volume. The third key technology is a blackbody calibration target fabricated with MDL's black silicon to have very high emissivity in a flat plate construction. JPL has completed design and breadboard of the mechanical, electronic and thermal subsystems for CIRAS payload including a HOT-BIRD FPA, with filters in a dewar and a breadboard of the electronics and scan mirror assembly. Blue Canyon Technologies, developer of the CIRAS 6U CubeSat, completed the Final Design Review for the spacecraft.

1. INTRODUCTION

Hyperspectral radiances measured from Low Earth Orbiting (LEO) infrared (IR) sounders including the NASA Atmospheric Infrared Sounder (AIRS)¹ on Aqua, and the Cross-track Infrared Sounder (CrIS) on the Joint Polar Satellite System (JPSS) have among the highest impact of any measurement type when assimilated into operational weather forecast models^{2,3,4}. LEO IR sounder radiances are used to retrieve temperature and moisture profiles with high vertical resolution.⁵ AIRS profiles have been used to validate water vapor distributions in climate models and confirm positive water vapor feedback to global warming.^{6,7} CIRAS is an instrument approach to achieve temperature and water vapor profiles using hyperspectral infrared in a 6U CubeSat⁸. Although originally intended to fly in space but descope due to cost reasons, much was learned about the design and development of the CIRAS approach during the past two years, including detailed design of the payload and spacecraft, and technology demonstration of key subsystems.

*Thomas.S.Pagano@jpl.nasa.gov, (818) 393-3917, airs.jpl.nasa.gov

The CIRAS payload approach uses a mix of commercial and JPL developed hardware. Industry partners include Ball Aerospace, IRCameras, and Blue Canyon Technologies (BCT). Figure 1 shows a conceptual layout of the CIRAS instrument and the major subsystems. The CIRAS is designed with three key JPL Microdevices Laboratory (MDL) technologies: 1) HOT-BIRD detectors, 2) MWIR Grating Spectrometer (immersion grating), 3) Black Silicon Blackbody. At this time, the design is near or at completion for all subsystems. Hardware subsystems developed to completion include the HOT-BIRD Focal Plane Assemblies (FPAs), the FPA out of band blocking filters, the Integrated Dewar Cryocooler Assembly (IDCA) (IR Cameras), the Camera Electronics, the cryocoolers and the cryocooler electronics. Assemblies still in breadboard stage include the Payload Electronics including the motor driver, housekeeping and power conversion. Assemblies at the final design stage include the Optics (Ball Aerospace) and the Spacecraft (BCT), both of which had their Final/Critical Design Reviews. The CIRAS mechanical design is complete at the PDR stage having completed the CAD design and structural analyses on the optics mounts (bipods), but not on the other mounts. Slits for the spectrometer were fabricated (from black silicon) and the grating substrates were fabricated and AR coated.

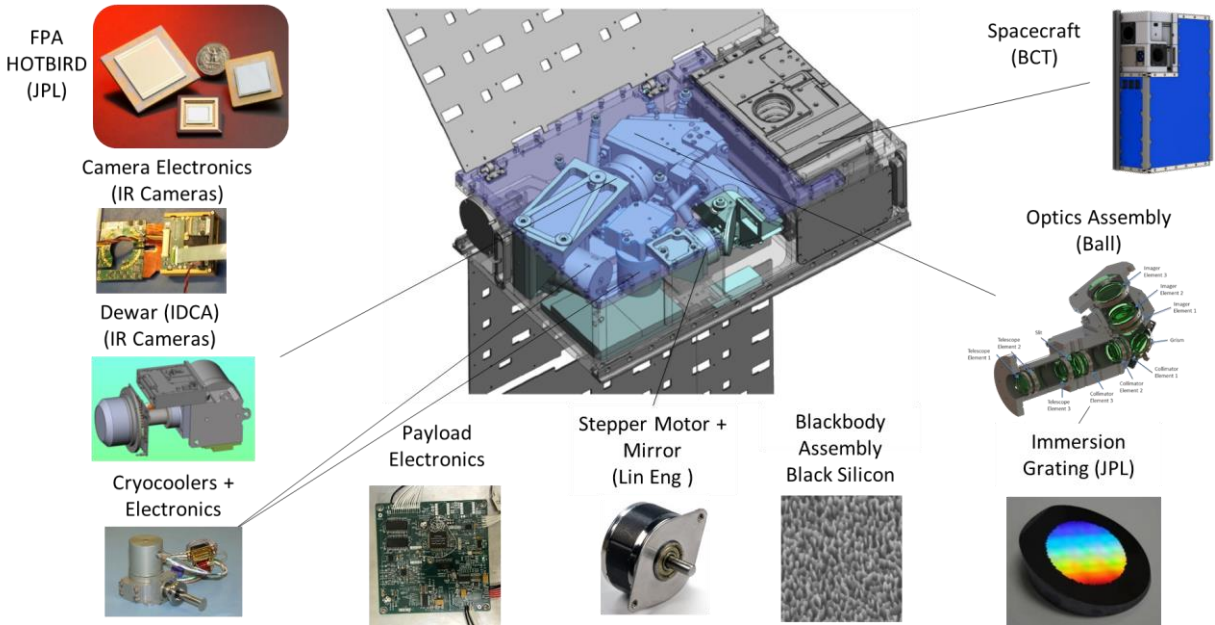


Figure 1. The CubeSat Infrared Atmospheric Sounder (CIRAS) and Major Subsystems.

2. SOUNDING REQUIREMENTS

Table 1 shows the performance capability of AIRS (similar for CrIS) compared to the requirements for CIRAS. The legacy sounders and CIRAS achieve relatively low spatial resolution, 13.5 km, but have a broad swath for global daily revisit. CIRAS orbit altitude is lower than AIRS and CrIS (between 450-600 km) contributing to a reduced swath. The pixel aggregation approach for CIRAS allows the same resolution to be achieved for any orbit altitude, and allows for higher resolution “zoom” mode. CIRAS zoom mode is not a requirement but enables testing the quality of higher spatial resolution (~3km) soundings over a smaller swath (~140 km).

A key requirement for CIRAS is that it fit in 6U CubeSat. This is intended to reduce the overall cost of

Table 1. AIRS Performance and CIRAS Requirements. CIRAS focuses on the lower troposphere.

Parameter	AIRS Performance	CIRAS Requirement
Vertical Range	0-<100mb	0-500 mb
Temperature Profile	≤1.5 K/km	≤1.5 K/km
Humidity Accuracy	15%/2km	20%/2km
Spectral Range	3.7-15.4μm	4.08-5.13μm
Spectral Resolution	≤0.5-2.2cm ⁻¹	≤ 1.2-2 cm ⁻¹
Spatial Res. (nadir)	13.5 km	13.5 km
Scan Range	1750 km	1500 km
NEdT	0.1-1.0K	<0.5K
Size	1.4 x 0.8 x 0.8 m ³	6U
Mass	177 kg	14 kg
Power	256W	35 W

the payload, satellite and launch making it useful as a gap mitigation system or to augment the currently available orbits. To meet a CubeSat volume we focus CIRAS on retrieval of temperature and water vapor profiles from the surface to the mid troposphere using only MWIR wavelengths. This allows for a smaller aperture, higher detector operating temperature and lower power operation. AIRS uses this band for retrieval of temperature in the operational product generation system due to its higher vertical resolution at lower altitudes. The disadvantage of this band is the higher variability of surface emissivity, and sensitivity to solar reflected energy from the surface, clouds and aerosols on the shorter side of the band. Solutions exist for many of these problems but more work is needed for operational use.

The spectral resolution of CIRAS is comparable to legacy sounders in this band providing similar vertical resolution in the lower troposphere⁸. The band includes 2 temperature sounding branches and goes well into the water continuum. Spectral range and resolution for CIRAS and the legacy sounders in this region are shown in Figure 2 along with a typical spectrum of the atmosphere (after convolution with the CIRAS Spectral Response Function (SRF)), highlighting the water vapor lines and CO₂ branch used for temperature sounding. We also show the AIRS channels used by the UK Met Office for data assimilation⁹. The legacy sounders achieve temperature sounding well into the stratosphere using the LWIR, although similar data in the stratosphere is achieved from microwave sensors. CIRAS is not meant to be a replacement of the legacy sounders that are expected to be in orbit for decades from now, but its value can be found in complementing these systems, and providing flexibility in orbit selection or constellations.

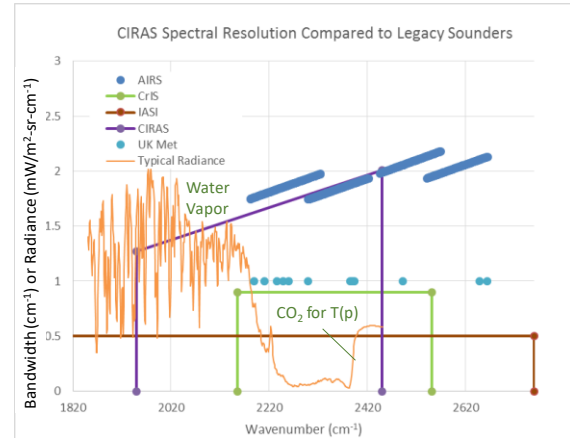


Figure 2. Spectral Resolution and Coverage for CIRAS compared to legacy IR sounders

3. CIRAS DESIGN OVERVIEW

3.1 Block Diagram

A block diagram of the CIRAS, color-coded to show completion status, is shown in Figure 3. The CIRAS payload includes a scan mirror capable of rotating 360° to view Earth, cold space and an internal blackbody for calibration. The scan mirror is driven by a high detent microstepper motor by Lin Engineering. Attached to the motor is an indexer that is used to determine the start position of each scan profile. The blackbody is a simple flat plate composed of black silicon mounted and instrumented with a temperature sensor. Black silicon offers very high emissivity in a compact flat plate construction

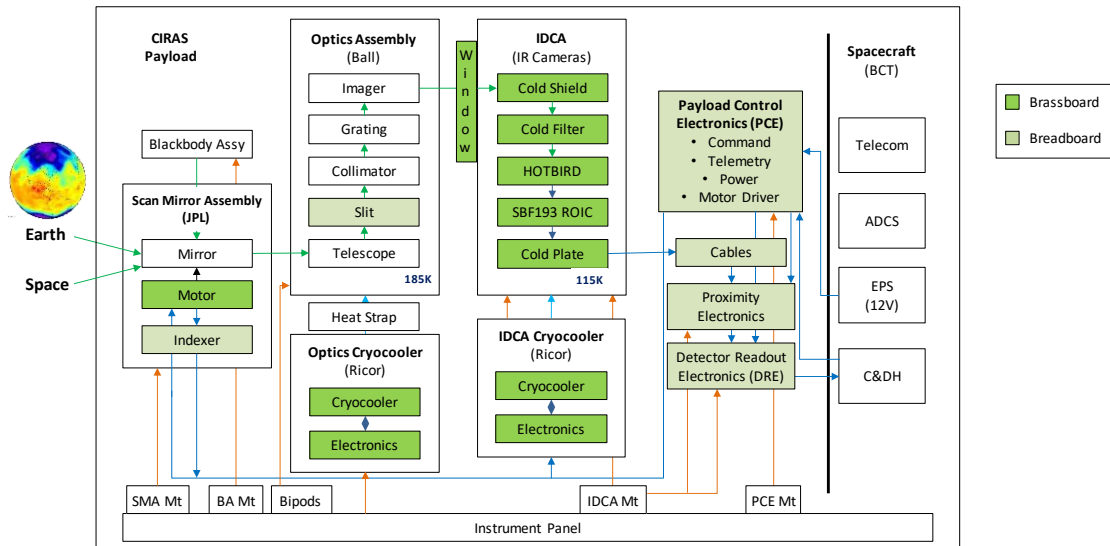


Figure 3. Block diagram of the CIRAS instrument.

and is more robust than carbon nanotubes. The CIRAS system is calibrated by viewing space and the on-board blackbody with the scan mirror before and after each Earth view.

Energy from the scan mirror is collected using an all-refractive telescope. Energy from the telescope is focused onto the entrance slit of an all-refractive MWIR Grating Spectrometer (MGS). The MGS covers the 4.08-5.13 μm spectral range in 625 channels and employs an immersion grating to reduce size and distortion. This band was selected because it contains a CO_2 absorption feature near 4.1 μm that can be used for temperature sounding and continues well into the water vapor continuum at longer wavelengths for water vapor sounding. The spectral response of the system resolves the absorption features with sufficient resolution to provide good vertical resolution of the profiles. The CIRAS optics will be developed by Ball Aerospace of Boulder Co. JPL will develop the immersion grating using e-beam etching technology and the entrance slit made of black silicon. The telescope and spectrometer are cooled to 185K using a Ricor K508N cryocooler heat sunk to the chassis.

The spectrometer disperses the energy across the spectral range and produces a 2-dimensional image at the focal plane with one direction spatial (504 pixels) and the other spectral (625 channels). The detector array uses the JPL HOT-BIRD photosensitive material hybridized on a Lockheed Martin Santa Barbara Focalplane (SBF) 193 Readout Integrated Circuit (ROIC). The ROIC is mounted in a standard Integrated Dewar Cooler Assembly (IDCA) developed by IRCameras. The IDCA provides vacuum, cold shielding and spectral filtering of unwanted out-of-band and ghosting energy. The detector is cooled to 115K using a second Ricor K508N cryocooler with cold tip contained within the IDCA and with the compressor heat sunk to the spacecraft instrument panel. Cryocoolers run autonomously once turned on from power directly from the spacecraft bus.

Clocks, biases and A/D conversion are performed using commercial electronics contained in a combination of the Proximity Electronics and Detector Readout Electronics (DRE). Detector signals from the DRE go directly into the spacecraft through a "Camera Link" interface. Payload Control Electronics (PCE) include motor control electronics that drive the scan motor, and the motor indexer electronics that control read the indexer. The PCE also reads housekeeping data including temperature sensors and provides power to the DRE. Electronics, cryocooler and spacecraft waste heat is dissipated into the spacecraft chassis through the instrument panel.

The CIRAS spacecraft will operate in a sun synchronous orbit at an altitude ranging from 400-600 km and provide 12V power at 2A supporting payload activation and operations. Current estimates indicate the spacecraft can provide 30 min of data per orbit on the night side due to power limitations. The current plan is for the spacecraft to use the Cadet UHF radio. Data collection is sized to match the data downlink capability. The spacecraft provides spatial and temporal binning of data from the FPA in the on-board computer to match the particular data acquisition mode. The pointing knowledge budget from all contributors of 0.3 pixels 1-sigma (1.6 mr in Zoom mode) is readily satisfied by the spacecraft. CIRAS can be placed in a variety of acquisition configurations including Global, Zoom, Pushbroom Zoom, Imagery and Winds modes. Some of these require changing the attitude of the spacecraft to support the acquisition.

3.2 Imaging and Scanning

The CIRAS employs pixel and frame averaging to achieve the desired size of the Field of View (FOV). The system can achieve low spatial resolution (13.5 km) with global coverage in "Global" mode, or high spatial resolution (3km) in a narrow swath in "Zoom" mode. Orbit, imaging and scan parameters are shown in table 2. CIRAS scans slowly through the Earth view (~20s) then rapidly (~1s) completes the revolution. The CIRAS imaging geometry is shown in Figure 4. One dimension is used for the spectrum and corresponds to the direction perpendicular to the length of the slit. The second dimension is used for spatial information, projecting a line onto the ground at nadir. A total of 625 channels and 504 spatial detector elements (pixels) are used respectively. In Global mode, the CIRAS adds 42 pixels along track and averages 8 frames while scanning cross-track to make a single FOV. The 42 pixels are averaged for every spectral channel. The slit projection is scanned cross-track, mapping the earth as the

Table 2. CIRAS Nominal Orbit, Imaging and Scanning Parameters

Orbit	Global	Zoom
Altitude (km)	600	600
Inclination (deg)	98.7	98.7
Ground Vel. (km/s)	6.91	6.91
Imaging	Global	Zoom
FOV (km)	13.44	2.88
N_FOVs_trk	12	56
N_Pixels_trk	504	504
Pixels/FOV_trk	42	9
Frames/FOV_xtrk	8	13
Scanning	Global	Zoom
Scan Efficiency	0.89	0.89
Swath_trk (km)	161	161
Swath_xtrk (+/-deg)	49.63	6.73
Swath_xtrk (km)	1522	142
Active Scan Time (s)	20.5	20.4
Scan Rate (r/s)	0.084	0.012
Tdwell (s)	0.267	0.433
Integration Time (s)	0.022	0.019

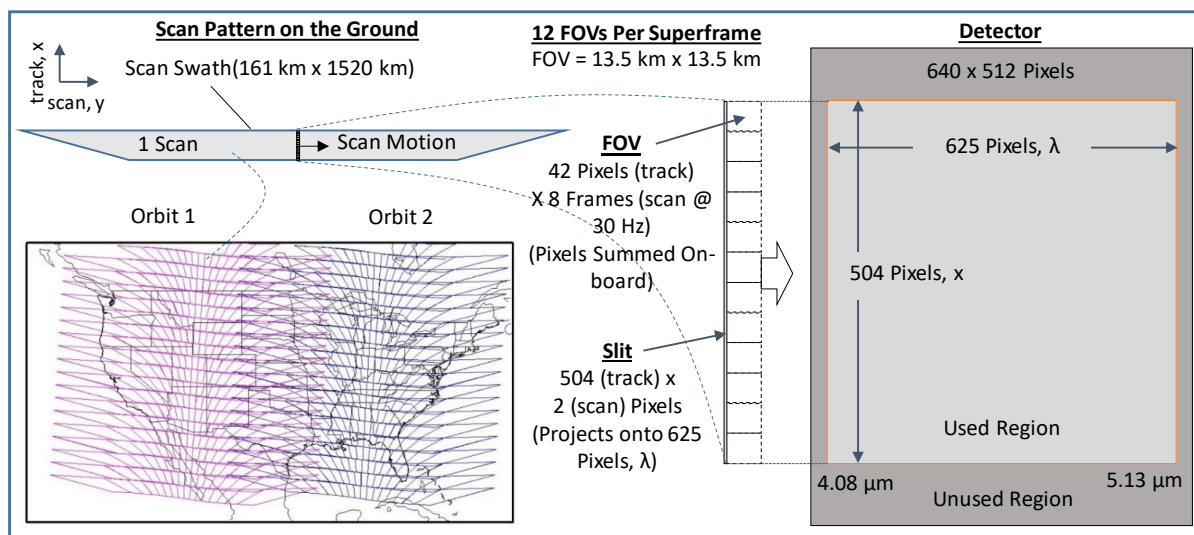


Figure 4. Scan pattern and projection on the ground and detector for CIRAS in global mode in a 600 km orbit. CIRAS makes 12 Fields of View (FOVs) by averaging 2 frames and 42 pixels along track per FOV.

satellite moves along the track direction. As the slit scans cross-track it rotates, however all spectral channels are co-registered by virtue of the slit. The scan rate and sampling rate are fixed for a given orbit to achieve 2 frames of data every 13.5 km footprint.

In scanning Zoom mode, the sensor will be able to achieve 3 km spatial resolution over a 142 km swath. In this mode, only 9 pixels and 13 frames are averaged per FOV. The additional frames are needed to improve SNR at the expense of a reduced swath. Wider swath in zoom mode may be possible depending on actual noise from the instrument and available data rate. In pushbroom Zoom mode the spacecraft is rotated and the scan mirror stationary producing a 161 km swath and more regular footprint as described below.

4. DATA ACQUISITION MODES

Figure 5 shows a set of typical acquisition modes that can test the ultimate limits of the CIRAS. Although we identify 5 modes below, there could be other modes of acquisition to achieve a different spatial resolution or swath.

Global (13.5 km)	Zoom (3 km)	Pushbroom Zoom (3 km)	BroadBand Imagery (1 km)	Winds (3 km)
<p>GSD = 13.5 km</p> <p>161km 12p 1522 km, 77p</p>	<p>GSD = 2.88 km</p> <p>161km 56p 142 km, 47p</p>	<p>GSD = 2.88 km</p> <p>161km 56p</p>	<p>GSD = 1.0 km</p> <p>161km 161p</p>	<p>GSD = 2.88 km</p> <p><161km <56p <142 km, <47p</p>

Figure 5. CIRAS can test multiple data acquisition modes. Here are a few examples. Orientation of slit shown in red for first scan in each case.

4.1 Global Mode

This mode achieves 13.5 km spatial resolution with global daily coverage and mimics the operational sounders currently flying. In this mode, the spacecraft is flying with the 1U x 2U side along the velocity vector and 1U x 3U side facing at nadir. The telescope projects the image of the slit onto the ground oriented lengthwise along track. As shown in Figure 4, the slit rotates with scan, but maintains good coverage. Binning occurs in the spatial direction (along track) and frame averaging occurs cross-track with the scan motion to make a full 13.5 km pixel.

4.2 Zoom Mode and Pushbroom Zoom Mode

Zoom mode achieves a smaller FOV over a smaller region to provide more soundings per unit area in these regions. It is achieved by slowing the scan rate in the Earth View and averaging a different number of pixels and frames. The scan is slow and long, with each 2.88 km FOV covered in 0.433 s. With the satellite moving at 6.9 km/s, the pixel is blurred along-track by 2.99 km. This produces a trapezoidal spatial response. A second zoom mode, called “pushbroom zoom” has no scan blur in the spatial direction and a more square response. In this mode the satellite is nadir Earth pointing and rotated in the yaw direction by 90 degrees with the scan mirror pointed at nadir orienting the slit perpendicular to the track direction.

4.3 Broadband Imagery Mode

Improving the spatial resolution to 1km is possible by binning fewer pixels. NEdT can be recovered by averaging pixels in the spectral direction, resulting in broader spectral bandwidth of the data. The reduced spectral resolution reduces vertical resolution, but may be sufficient for land thermal imaging including fire detection and carbon monoxide transport.

4.4 Winds Mode

Atmospheric Motion Vector (AMV) winds mode is possible by tracking water vapor features in two successive images obtained over the same space on the ground separated in time. This has been successfully demonstrated in GOES and MODIS Imagery. Since CIRAS measures the 3D profile of water vapor, it is expected that two successive images by a CIRAS sounder could produce 3D AMV winds. Since we only have one satellite, in winds mode, the satellite points forward 30°, acquires data for 51.2 s, points nadir, acquires data for 51.2 s, then backwards 30° for the same time, acquiring 3 successive images of the same region on the ground. This technique can be used in either of the zoom modes. At this resolution and time interval, wind speeds would have to be in excess of 200 km/hr (hurricane) to be detected, but an experiment using CIRAS can help identify error sources in the AMV process.

4.5 Spectral / Spatial Mixing Correction

The CIRAS takes advantage of a large 2D focal plane to relax alignment requirements. In order to benefit from this feature, a signal processing algorithm, called “electronic alignment” is used to reformat the data. The grating spectrometer works by dispersing the energy in the cross-slit direction. Any rotation of the dispersion direction relative to a row of detectors will result in a spatial point on the slit mapping onto multiple rows. Uncorrected this could result in spatial-spectral mixing. We can correct for this by selecting the rows we average for each spatial element (FOV). For example, in zoom mode, we average 9 rows of detectors (along-track) for each 3 km FOV. The correction would allow these 9 rows to be different for each spectral position along the detector array.

5. CIRAS DESIGN AND DEVELOPMENT STATUS

The CIRAS project completed the preliminary design for all subsystems and the final design for several. Hardware delivery was made of the flight IDCA including the focal plane assembly, 2-band blocking filter, cryostat, Ricor cooler, proximity and camera electronics. The IDCA is a fully functioning camera that operates in ambient. Three additional Ricor cryocoolers were successfully procured for flight use. One of these is intended for cooling the optics and the other two are spares. The optics assembly completed the subsystem CDR, procured the optical elements, and completed the mechanical drawings. The vendor providing the optical elements has procured the material. JPL has completed the interface drawing and fabrication of the slit. The interface drawing for the grating was also complete but work has not yet started on the fabrication at JPL. JPL completed the breadboard for the PCE and demonstrated the ability to control the scan motor to the required rates. The thermal design of the system is complete with all operational temperatures identified, and shows we can meet thermal balance in orbit. The mechanical design is at the preliminary design level in that while the CAD design is complete, structural/thermal analyses are not complete and the mounts have not been fabricated. The scan motor was procured for flight use, and the scan mirror mount is designed but not procured. BCT completed the spacecraft Final Design Review and all ICDs.

5.1 HOT-BIRD Detectors

CIRAS uses a 512 x 640 element 24 μm pitch JPL High Operating Temperature Barrier Infrared Detector (HOT-BIRD). The HOT-BIRD technology is based on III-V compounds and offers a breakthrough solution for the realization of lower dark current and improving uniformity and operability compared to II-VI material (MCT) at lower cost. Low 1/f noise and high temporal stability allows CIRAS to use a slow scan for better sensitivity and less frequent calibrations¹⁰. Figure 6 shows a photo taken using the CIRAS HOT-BIRD detectors. The image reflects the high operability and good sensitivity of the device. The Readout Integrated Circuit (ROIC) chosen for the CIRAS detector was the SBF193 by Lockheed Martin. 56 FPAs, consisting of the detector hybridized to a ROIC, were successfully fabricated on the first lot demonstrating the high producibility of the process. Of these 5 were delivered for thinning and testing.

The FPA chosen to be placed in the IDCA for CIRAS was serial number 17CIL21. The FPA exhibits good connectivity at room temperature with very few poorly connected pixels. The FPA was tested at two operating temperatures 130K and 115K. The CIRAS FPA performance requirements and expected capability are shown in Table 3.

Detector	Requirement	Expected Capability	Rationale
Pixel Size (μm)	24 \pm 1	24	SBF-193 ROIC ICD
Spectral Range (μm)	4.08-5.13 \pm 1%	2 – 5.5	Device result
Quantum Efficiency @4.1 μm	> 0.35	~0.4	Device result
Operability	> 0.95	> 0.999	FPA result
Dark Current (A/cm^2)	<7.57e-07	< 3e-07	FPA result
Frame Rate (Hz)	30.0 \pm 10%	< 88 (max)	SBF-193 ROIC ICD
ROIC Saturation (e-)	> 8e+06	8.4e+06	SBF-193 ROIC ICD
ROIC Noise (e-)	< 600	< 500	SBF-193 ROIC ICD
Operating Temperature	< 115K	115K	Device/FPA result

Table 3: CIRAS HOT-BIRD FPA performance requirements and measurements.



Figure 6. An image taken with a HOT-BIRD FPA developed for CIRAS

5.2 Integrated Dewar Cryocooler Assembly (IDCA)

The FPAs are mounted in an evacuated dewar called the IDCA. The completed flight IDCA is shown in Figure 7. As mentioned above the IDCA provides not only the vacuum environment but includes the cryocooler for the detector and cold filters for blocking Ghosting and out-of-band light. The IDCA also includes the proximity board (shown in Figure 8) that provides clocks, biases and A/D to the FPA and the AgileCore camera electronics that provide power and data formatting for the Camera Link output. Early in the design phase we recognized that the MGS will produce a small amount of ghosting that can introduce spectral mixing of energy in the spectrometer. Cold filters were designed to mitigate the problem and essentially pass only energy for half the spectrum over the corresponding half of the focal plane. One cold filter passes 4.0-4.6 μm and rejects everything out of this band (from 1.5-4.0 μm and 4.6-6.5 μm), while the other filter passes the 4.6-5.2 μm and rejects similar to the other filter. These filters are mounted on the cold plate directly over the detector and together provide the necessary out-of-band blocking and ghosting reduction required by the system. The filter spectral response is shown in Figure 9. This plot was made by graphically overlaying the individual response of the two filters. We see from the plot that the required spectral band is passed and that both filters have .90% transmission at the seam of 4.6 μm . Both filters block outside their band from 2-6 μm allowing rejection from stray solar in the shortwave side, and excessive background flux

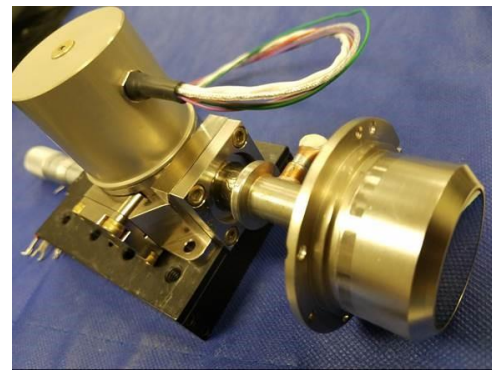


Figure 7. CIRAS IDCA. The IDCA holds the detector in an evacuated dewar and provides cooling, spectral blocking, and readout of detector signals

from the optics on the longwave side. The two band filter improves SNR on the shortwave half by blocking background energy from the longer wavelengths. The warm operating temperature of the IDCA window is of primary concern as it is the largest contributor to the background at the detector. The window is AR coated silicon with a theoretical emission of less than 0.4%, but further testing is required to determine if the background levels are sufficiently low at normal operating temperatures to minimize integration time windowing.



Figure 8: CIRAS Proximity electronics, DRE and flex cable.

The IDCA was designed to withstand vibration levels consistent with the General Environmental Verification Specification (GEVS) (14.1 grms), but only required to undergo a workmanship vibrate to reduced levels (6.8 grms). A mass equivalent IDCA was fixtured and exposed to X, Y, Z axis random vibration and shock. The unit survived all exposures verifying the design. The model was built with a glass piece with mass similar to the FPA and it doesn't have a dewar cap, but otherwise it is fully representative of the flight unit.

The parts list for the camera electronics were reviewed by the JPL parts group and it was found that Single Event Latchup (SEL) sensitive parts existed on both the proximity electronics and the power board. 10 parts on the proximity electronics have a sensitivity of 1 SEL / 100 days, and 3 parts on the power board had a sensitivity of 1 SEL / 10 days. For future flight, it was found that Digitrack electronics should be able to build a flight version of the electronics without high SEL sensitive parts for this FPA.

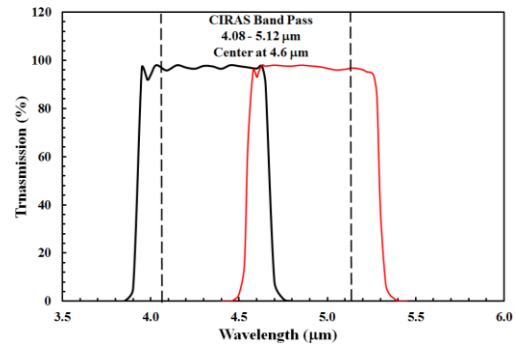


Figure 9: CIRAS IDCA blocking filter response

5.3 MWIR Grating Spectrometer (MGS)

The CIRAS MGS is a grating spectrometer based on designs developed by JPL and Ball Aerospace in the late 1990's and mid 2000's¹¹. The CIRAS MGS consists of the camera, the collimator and the telescope, comprise the bulk of the CIRAS optical system as shown in Figure 10. The Spaceborne Infrared Atmospheric Sounder (SIRAS) and SIRAS-Geosynchronous Earth Orbit (SIRAS-G) demonstrated wide field all refractive grating spectrometer systems operating in the LWIR and MWIR respectively with spectral resolution and field of view comparable to the CIRAS. CIRAS is different in that it employs a silicon immersion grating developed by JPL. The immersion grating provides higher dispersion and allows more favorable reflecting angles enabling a smaller spectrometer. Lens materials consist of Silicon, Germanium and IRG 25 and the design is athermal, allowing for alignment at room temperature while maintaining that alignment at the operational temperature of 185K. The slit is similar to those developed by JPL for other spectrometer projects darkened with black silicon. The optics performance is predicted to be excellent with near diffraction limited image quality, better than 50% transmission and less than 30 μm distortion at the FPA.

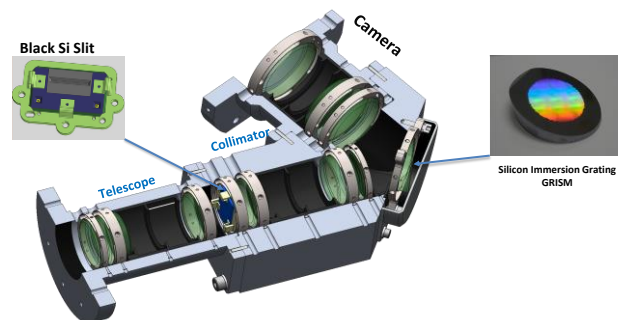


Figure 10: CIRAS Opto-Mechanical Design

During the design phase, several issues were found with the optics that needed resolution. The first was that a significant amount of ghosting ($>10^{-3}$) is present in the system that results from reflections off the lenses and grating. The ghosting was analyzed at multiple wavelengths and it was found that shortwave energy was being passed to the longwave side of

the FPA and longwave energy was being passed to the shortwave side of the FPA. Analysis indicated that including a 2-band filter on the FPA, and imposing a strict requirement on the AR coatings ($>0.25\%$) would reduce the ghosting by an order of magnitude or more. Finally, the grating first surface was angled slightly more than nominal to reflect the energy off the FPA by 1.5 mm. The cold shield was designed to block this energy from striking the FPA. Another major concern during the design phase was the packaging of the optics; the initial design did not fit in the CubeSat volume. The optics were redesigned at Ball to shorten the EFL of the telescope and collimator achieving an overall reduction along this dimension of 30 mm. This reduction was significant enough to solve the packaging problem with the optics.

At this time, the optical design structural and thermal analysis are complete and all mechanical drawings are complete including the mechanical ICDs and drawings for the slit and the grating. The procurement specification for the lenses is complete. The immersion grating substrates were on a separate contract and were completed: 8 grating substrates were delivered to JPL, 4 coated with better than 0.5% reflection (0.2% required), and 4 uncoated. See photo of substrates received in Figure 11. The vendor, ISP, was unable to achieve the 0.2% reflectance required, but the coated parts are usable in a future CIRAS flight system as is after grating ruling. JPL also fabricated prototype slits of black silicon for the spectrometer (Figure 12). Three potentially usable parts were made pending backside metallization. The parts exhibit some cosmetic damage due to over etch of the perimeter oxide on the front side.

5.4 Mechanical Design

The mechanical design for CIRAS is shown in Figure 13. Packaging the required components into a 2U x 2U x 1U (20 cm x 20 cm x 10 cm) payload allocation turned out to be particularly challenging. Firstly the optical design requires two fold mirrors between the scanner and telescope in order to orient the beam. These fold mirrors protruded outside the volume in the original design. As mentioned above, a redesign by Ball of the telescope and collimator reduced the overall length to just fit within the volume. JPL developed a mounting approach for the spectrometer using “bipods” that achieve a high degree of thermal isolation and mechanical rigidity while fitting within the package. All subsystems are mounted to the spacecraft “instrument panel” which is a 2U x 3U plate of aluminum on the space side of the spacecraft that closes off the 6U CubeSat enclosure. This makes integration and test of the payload with the spacecraft easier.

In early designs, the spectrometer was attached to the IDCA so the spectrometer would maintain alignment with the focal plane as the structure distorts with temperature or other factors. While technically feasible, this approach turned out to be more costly than the project could afford due to the complexity of the design. Additionally the higher thermal load on the spectrometer from the hot IDCA exterior, even with isolation, turned out to be too great a load on the optics cryocooler. A simpler approach was adopted where the IDCA and spectrometer are independently mounted and aligned to each other using shims. The approach could ultimately lead to displacements of the spectrum during launch (from its position during ground calibration), as well as in orbit with thermal fluctuations. We plan to remove spectral errors



Figure 11. CIRAS Grating Substrates

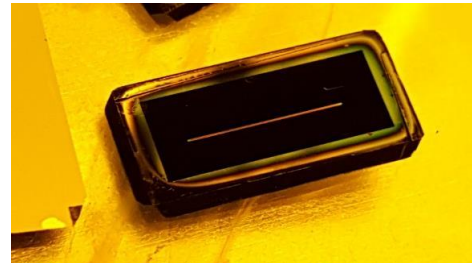


Figure 12. CIRAS Slit from the 1st Wafer

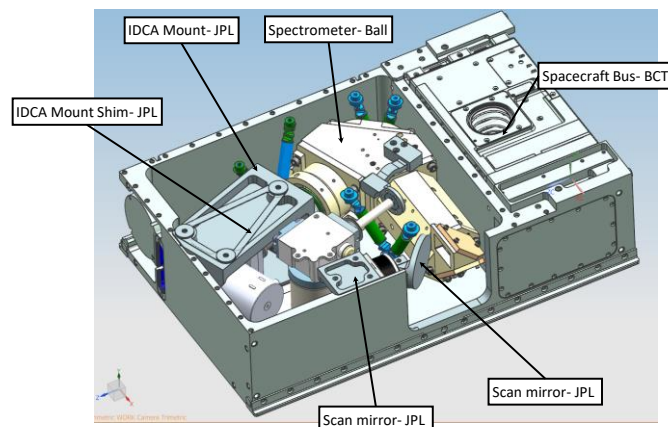


Figure 13. CIRAS Mechanical Design

during ground processing by recalibrating the spectrum to atmospheric absorption lines. We also can remove spatial misalignments by choosing the pixels we use to make a FOV during the binning process as mentioned above in the process called “electronic alignment”. Retrofitting the instrument with a detector mount that mounts directly to the optics is preferred at some point in the future.

The detailed design of the mounts started late in the task due to the design and packaging issues described above, but a final concept is complete with all subsystems fitting in the 4U allocate volume. Three bipod mounts consisting of modified G10 OTS tubing truss members with Ti6Al4V end fittings and integrated flexures provide good thermal isolation and rigidity of the assembly. The IDCA mount and scan mirror mount designs use 6061-T6 aluminum alloy and fasten to the instrument panel. They are aligned to the optics using shims with bond pad features for shear location. The optics cryocooler mounts directly to the instrument panel. Finally the heat strap is all aluminum with end fittings that bolt to the spectrometer and cold tip of the cryocooler. The electronics and blackbody target mounts are not complete but are expected to be straightforward.

A mass estimate for the CIRAS is given in Table 4. The values in the table are Maximum Expected Value (MEV). With an anticipated spacecraft mass of 8.88 kg, the total MEV instrument mass (payload + spacecraft) is estimated to be 13.6 kg.

5.5 Thermal Design

The thermal requirements for CIRAS are among the most challenging of all requirements for the system. The requirements call for maintaining the detector temperature at 115K, and the optics at 185K. This is achieved using two active cryocoolers, one cooling the detector in the IDCA and the other cooling the optics housing. The spectrometer is thermally isolated using G10 bipods. MLI will surround the spectrometer for thermal isolation. Early in the design, passive cooling of the optics was considered however, the cost of the design and development of a new passive cooler were considered to be too high for CIRAS. Heat generated by the cryocoolers and electronics is transferred to the spacecraft structure which in turn radiates heat to space. Silver Teflon tape (10mil) will be used on the spacecraft structure to maximize radiating efficiency for all sun angles. Survival heaters will be used when needed in order to keep temperatures at a safe level. Thermal analysis by BCT indicates they can meet the requirements that the instrument panel temperature be maintained between the required -10C and +40C during turn on/off and normal operations with better than 15C margin.

Figure 14 shows the key elements of the CIRAS thermal model. In order to bound the environmental design, analysis was performed for extreme solar cases of Low Earth Orbit (LEO). “Beta zero” and “beta 90” solar incidence angles relative to the orbit plane would represent the extremes. Note: A 10:30 AM A-train orbit was also analyzed and results did not vary much from an operational hot scenario. The thermal model uses power emission estimates for the major subsystems. Masses and surface properties are based on best estimates for the design.

Allowable flight temperatures resulting from the model analysis and parts sensitivity are shown in Appendix C. Model analysis shows it will take about 50 hours to cool the optics from a temperature of 293.15K to 185K. Cooling margin for the optics cooler is 24%. It will take less than 1 hour to cool the FPA from 293.15K to 115K. Cooling margin for the FPA is 200%. The high margin in the FPA allows for a lower

Table 4. CIRAS Payload Mass

Payload Item	Tot MEV (g)
IDCA	438
IR Camera electronics	73
FPA cryocooler	500
Optics Assembly	1703
Fold Mirrors	18
Fold Mirror mounts	63
Payload Control Electronics (PCE)	63
Optics cryocooler	500
Thermal hardware	63
Thermal straps	58
Thermal interface electronics	13
Scan mirror	14
Calibration Target	3
Motor	144
Motor controller	63
Fasteners	125
Cabling/Harness	375
Structures	350
Spacecraft Structure Coatings	13
Total Payload Mass	4574

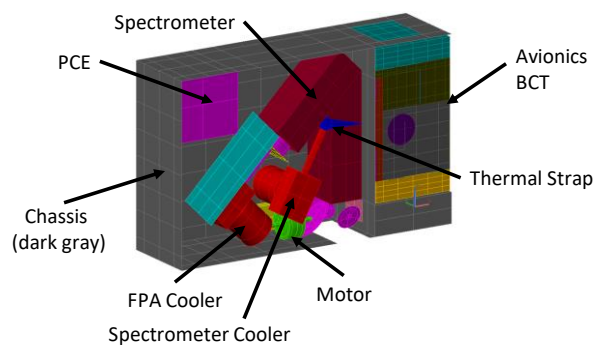


Figure 14. CIRAS Thermal Model

operating temperature if needed but at this time the noise is driven by the optics background flux not the dark current so lower FPA temperatures may not significantly improve overall noise.

The CIRAS thermal design decouples the optics from the IDCA since the optics need to run cold and the IDCA operates hot (about 305K). The design is not optimal for a thermal infrared instrument since the hot window of the IDCA introduces background loads that are greater than that produced by the emission of the optics. The consequence is higher NEdT of the measurement. If the optics were attached to the IDCA, the temperature of the optics would rise but the IDCA window would be colder. Analysis shows if the IDCA and optics were attached, the temperature of the optics would rise to 215K, while the window would also achieve that temperature. Figure 15 compares the NEdT for the hot window/cold spectrometer with the cold window/warm spectrometer. It turns out that both of these cases give about the same NEdT; this information may be useful as we should allow for coupling the two in the event more margin exist in the optics cryocooler that we could use to reduce window and optics temperature. The ideal case of cold window/cold optics are also shown in the figure to demonstrate the true potential of the instrument if the window can operate cold.

5.6 Cryocooling

The CIRAS will use the Ricor K508N cryocooler shown in Figure 16. This cooler has the best performance for its mass, volume and input power. It has high cooldown capacity and fits in the 4U cubesat volume. It is low cost and drive electronics fit inside the cooler mount housing making it easy to operate. Battery power is sufficient to keep both coolers operating continuously throughout the mission. Ricor has stated the Mean-Time-To-Failure (MTTF) for the K508N cooler is ~20,000 hours operating under “standard working conditions” (undefined phrase used by Ricor). This would enable at least a year and a half operation in orbit. The K508N has improved bearing lubricants and improved hermetic seals. These cryocoolers flew on the MSL/CheMin and DAWN missions. Exported Vibe, DC and AC Magnetics were measured for a sample cryocooler and no issues were found with other parts of the system. Ricor performed thermal test and exported vibe test of the cherry-picked coolers. This helped identify which coolers to use for the 115K FPA and for the 185K Spectrometer.

5.7 Electronics Design and Brassboard Testing

The CIRAS electronics consists of several independent boards providing unique functions for the payload (please refer to Figure 3). The Payload Control Electronics (PCE) provides four primary functions: a) communications between the payload and the spacecraft, b) sensing instrument telemetry and relaying to the spacecraft c) power and control of the scan motor, d) power regulation for the Detector Readout Electronics (DRE). The final design was selected from several alternates considered during the design phase. The first alternate was a custom electronics FPGA to provide all communications and data handling from the focal plane. Later it was realized that the spacecraft can accept “Camera Link” input directly from the DRE. This obviated the necessity for the payload to handle the data, greatly reducing requirements on the PCE. Next a separate motor controller and housekeeping boards were considered to handle those functions along with of the TEMPEST-D microprocessor board for the payload control and remaining payload control

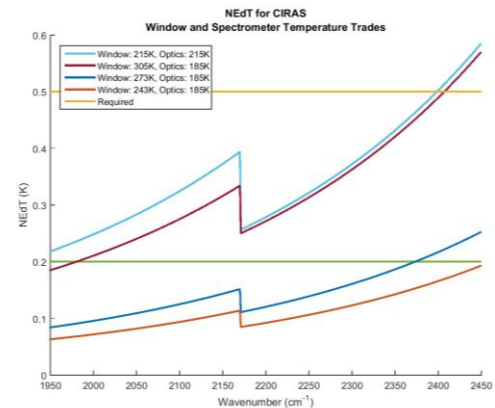


Figure 15. CIRAS NEdT for different window and optics temperatures

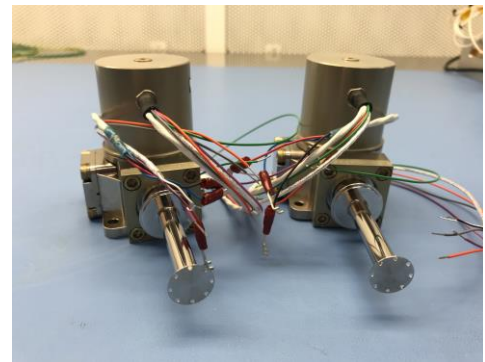


Figure 16. Ricor K508N Cryocoolers purchased for CIRAS

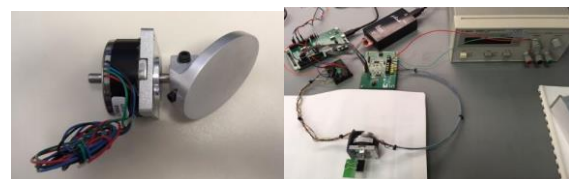


Figure 17. (Left) Scan motor with breadboard scan mirror substrate. (Right) Motor control test setup

functions. Experiment with a Vorago microcontroller used for testing the scan profile (see Figure 17) led to the design of a single board with the all PCE functions described above. The board is smaller than the stack of 3 boards required with the TEMPEST-D approach as shown in Figure 18 (left). The new board was developed as a breadboard and tested and is shown Figure 18 (right). Motor control functions were demonstrated with the new board to the required rates, as well as the functionality of the housekeeping capability. The power required by the payload in normal data acquisition mode is 23.2 W. A breakdown of the predicted power for the system for the in-flight modes is given in Table 5.

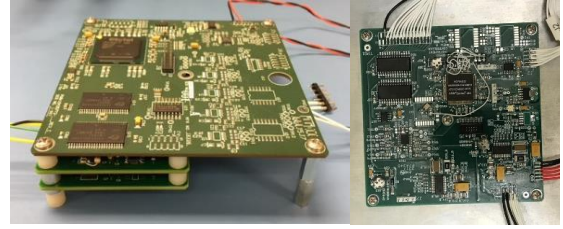


Figure 18. (Left) CIRAS 3-board PCE breadboard (early approach), (Right) CIRAS 1-board PCE breadboard (final approach).

Clocks and biases and A/D conversion for the SCA are provided in a small board next to the dewar called the Proximity Electronics. Digital data from the Proximity Electronics are multiplexed through the DRE which, as mentioned above, provides a Camera Link output that feeds directly into the spacecraft C&DH system. Cryocoolers are operated directly from the spacecraft bus.

At this time we have also completed a cabling diagram and brassboard cables for testing the electronics. The next steps include completion of the PCE testing, flight fab of the PCE and cables, integrating with the flight DRE, full payload system electronics testing and integration and test with the spacecraft. A separate brassboard DRE was purchased to send to BCT for testing receipt of the camera data through the camera link interface.

Table 5. CIRAS Power Estimate

System	Item	CBE Power (W)	Contingency	MEV Power (W)	Power (Watts)						
					Safe	Warm Standby	Optics Cool down	FPA Cool down,	Cold Standby	Data Collect	Down-link
					24 hrs	24 hrs	36 hrs	1 hrs	24 hrs	TBD	~10 min
Payload	Payload Control Electronics	0.65	30%	0.85	0.00	0.78	0.78	0.78	0.78	0.85	0.78
	Motor	0.25	30%	0.33						0.33	
	Motor Indexer Electronics (MIE)	0.04		0.04						0.04	
	Detector Readout Electronics	3.74	30%	4.86	0.00	0.00	0.00	0.00	0.00	4.86	0.00
	Proximity Board	0.10	30%	0.13	0.00	0.00	0.00	0.00	0.00	0.13	0.00
	Optics Cryocooler (Cooling)	10.00	5%	10.50	0.00	0.00	10.50	--	--	--	--
	Optics Cryocooler (Steady-State)	10.00	5%	10.50	0.00	0.00	--	10.50	10.50	10.50	10.50
	FPA Cryocooler (Cooling)	10.50	5%	11.00	0.00	0.00	--	11.00	--	--	--
	FPA Cryocooler (Steady-State)	6.00	8%	6.50	0.00	0.00	--	--	6.50	6.50	6.50
				Payload Sub-total	0.00	0.78	11.28	22.28	17.78	23.20	17.78
S/C	SC boards: Power and Processor	3.57		3.57	3.57	3.57	3.57	3.57	3.57	3.57	3.57
	Reaction Wheels	0.40		0.40	0.40	0.40	0.40	0.40	0.40	0.40	0.40
	Star Trackers	0.83		0.83	0.83	0.83	0.83	0.83	0.83	0.83	0.83
	Magnetorquers	0.23		0.23	0.23	0.23	0.23	0.23	0.23	0.23	0.23
	GPS	0.10		0.10	0.10	0.10	0.10	0.10	0.10	0.10	0.10
	Radio Rx	0.30		0.30	0.30	0.30	0.30	0.30	0.30	0.30	0.30
	Radio Tx	11.00		11.00	0.00	0.00	0.00	0.00	0.00	0.00	11.00
	SC Heaters for Payload	21.00		21.00	18.0	21.00	11.00	0.00	0.00	0.00	0.00
				TOTAL:	23.43	27.21	27.71	27.71	23.21	28.63	34.21

5.8 Spacecraft

The CIRAS spacecraft design is a 6U XB1 by Blue Canyon Technologies (BCT). The XB1 includes the Attitude Determination and Control System (ADCS), including 3-axis stellar attitude determination, low-jitter reaction wheels, torque rods and integrated control algorithms. The XB1 Command and Data Handling (C&DH) system receives data from the payload and provides autonomous operation of the system. The XB1 flight software provides stored commands and macros, attitude determination and control, orbit propagation, modeling of orbital parameters, reaction wheel control, and a host of other functions. The flight software for CIRAS would bin the focal plane data into the desired resolution and perform the electronic alignment of the data prior to sending to the ground. The XB1 Electrical Power System (EPS) board provides spacecraft electrical power control and distribution. The solar panel configuration is a 2-wing configuration (see Figure 19) with 14 strings and 8 cells per string. This gives a conservative estimate of 98W to the system during charging.

With this power, the CIRAS is able to keep both coolers operational at all time and collect data for 30 minutes every orbit on the eclipse side. The spacecraft is oriented to charge the panels during the sunlight portion of the orbit. For communications, the CIRAS spacecraft uses a Cadet UHF radio and a deployable monopole antenna similar to those completed on multiple BCT spacecraft. Table 6 gives the anticipated data rate and downlink capacity of the system. For global mode, all data that can be acquired (30 min/orbit limited by the power system) can be downloaded. For zoom mode, only 14.6 minutes of data can be downloaded per orbit. This assumes all channels are downloaded. (Note: less than 100 channels are necessary to download to perform a temperature and water vapor retrieval). Finally, for GPS, the Novatel OEM719 or the latest model is utilized and communicates directly with the attitude determination and control system to optimize the position solution.



Figure 19 CIRAS Spacecraft uses a 2 wing configuration providing over 98W during charging

6. SUMMARY AND CONCLUSIONS

The CIRAS is an instrument approach for a hyperspectral infrared sounder operating in the MWIR in a 6U CubeSat. CIRAS incorporates new component technologies including a wide field spectrometer employing an immersion grating, HOT-BIRD detectors, and a Black-Silicon blackbody all developed at JPL's Microdevices Laboratory (MDL). These new technologies combined with an ESTO heritage spectrometer developed by Ball Aerospace, commercial camera technologies from IR Cameras, flight proven low-cost high performance Ricor Cryocoolers, and a proven BTC 6U spacecraft enable the CIRAS to be developed with relatively low cost and risk. At this time, the HOT-BIRD FPAs have been successfully fabricated and integrated into the Integrated Dewar Cryocooler Assembly (IDCA) which is also complete and contains the FPA,

optical blocking filters, cold shield, dewar window, vacuum enclosure and cryocooler. The IDCA electronics are complete and the CIRAS PCE have demonstrated scan profile motion. The electronics are in the brassboard stage and the optics are ready for fabrication. The CIRAS spacecraft has successfully completed the Final Design Review.

Table 6. CIRAS Data Rates and Download Capacity

Parameter	Global-13.5 km	Zoom - 3 km
Orbit Period (s)	5792.0	5792.0
Number of Spectral Channels	625	625
Number of Spatial Pixels	504	504
Frame Time	0.03333	0.03333
Quantization Bits	14	14
Data Compression Factor	1.00	1.00
Raw Data Rate (Mbps)	132.3	132.3
Number of Superpixels Along Track	12	56
Number of Channels to Download	625	625
Frames to Average	8.0	13.0
Telemetry & Overhead (Mbps)	0.10	0.10
Aggregated Data Rate (Mbps)	0.49	1.23
Minutes of Data to Download (min)	30	30
Data Volume Per Orbit (Gb)	0.89	2.22
Downlink Time / Pass (min)	6	6
Downlink Rate (Mbps)	3	3
Downlink Capacity Per Orbit (Gb)	1.08	1.08
Percentage of Data Downloaded (%)	121.5	48.8
Minutes of that can be downloaded (min)	36.5	14.6

ACKNOWLEDGEMENTS

The research was carried out at the Jet Propulsion Laboratory, California Institute of Technology, under a contract with the National Aeronautics and Space Administration. The authors would like to thank our sponsors at NASA Earth Science Technology Office including George Komar, Pam Millar, Charles Norton, and Sachidananda Babu for their leadership and support. We would like to thank the NOAA Office of Projects, Planning and Analysis (OPPA), in particular Margaret Caulfield, David Furlong, Dan Mamula, Joanne Ostroy and Jacob Inskeep, for collaborating with us on their Earth Observing Nanosatellite-Infrared (EON-IR) design study. In particular much of the work presented here in the electronics, scanning and thermal design was performed for the EON-IR study and was directly applicable to CIRAS.

Reference herein to any specific commercial product, process, or service by trade name, trademark, manufacturer, or otherwise, does not constitute or imply its endorsement by the United States Government or the Jet Propulsion Laboratory, California Institute of Technology. © 2018 California Institute of Technology. Government sponsorship acknowledged.

REFERENCES

- [1] Pagano, T. S., M.T. Chahine, E.J. Fetzer, “The Atmospheric Infrared Sounder (AIRS) on the NASA Aqua Spacecraft: a general remote sensing tool for understanding atmospheric structure, dynamics and composition” Proc. SPIE 7827-11, (2010).
- [2] Cardinali, C, “Monitoring the observation impact on the short-range forecast” QJR Met Soc 135, 239–250 (2009)
- [3] J. Le Marshall, J. Jung, M. Goldberg, C. Barnett, W. Wolf, J. Derber, R. Treadon and S. Lord, “Using cloudy AIRS fields of view in numerical weather prediction” Aust. Meteorological Magazine 57, 249-254 (2008).
- [4] McNally, A.P., Watts, P.D., Smith, J.A., Engelen, R., Kelly, G.A., Thepaut, J.N., and Matricardi, M., “The assimilation of AIRS radiance data at ECMWF” QJR Meteorol. Soc. 132, 935-957. doi: 10.1256/qj.04.171 (2006).
- [5] Susskind, J., J. M. Blaisdell, and L. Iredell, “Improved methodology for surface and atmospheric soundings, error estimates, and quality control procedures: the AIRS science team version-6 retrieval algorithm” J. Appl. Remote Sens. 8(1), 084994 (2014).
- [6] Pierce D. W., T. P. Barnett, E. J. Fetzer, P. J. Gleckler, “Three-dimensional tropospheric water vapor in coupled climate models compared with observations from the AIRS satellite system” Geophys. Res. Lett. 33, L21701, doi:10.1029/2006GL027060. (2006).
- [7] Dessler, A. E., Z. Zhang, and P. Yang, “Water-vapor climate feedback inferred from climate fluctuations, 2003-2008” Geophys. Res. Lett. 35, L20704, doi:10.1029/2008GL035333. (2008)
- [8] Pagano, T. S., D. Rider, M. Rud, D. Ting, K. Yee, “Measurement approach and design of the CubeSat Infrared Atmospheric Sounder (CIRAS)”, Proc. SPIE 9978-5, San Diego, CA (2016)
- [9] Saunders, R. W., et al., “Monitoring satellite radiance biases using NWP models” IEEE TGRS 137 (2012)
- [10] Gunapala, Sarath, et al., “1/f Noise QWIPs and nBn Detectors” Proc. QSIP (2014)
- [11] Kampe, T., T. Pagano, J. Bergstrom, “SIRAS, The Spaceborne Infrared Atmospheric Sounder: an approach to next-generation infrared spectrometers for Earth remote sensing” Proc. SPIE 4485 (2002).